Heteroepitaxial Growth of Nanostructured Cerium Dioxide Thin Films by MOCVD on a (001) TiO_2 Substrate

Raffaella Lo Nigro,[†] Roberta Toro,[‡] Graziella Malandrino,[‡] and Ignazio L. Fragalà*[,‡]

Dipartimento di Scienze Chimiche, Università di Catania, and INSTM, UdR Catania, Viale A. Doria 6, 95125 Catania, Italy, and IMM, sezione di Catania, CNR, Stradale Primosole n 50, 95121 Catania, Italy

Received November 5, 2002. Revised Manuscript Received January 6, 2003

The deposition of epitaxial CeO_2 nanostructured thin films on rutile (TiO_2) substrates by metal−organic chemical vapor deposition (MOCVD) has been carried out in a wide temperature range. Films have been grown on (001)TiO_2 from the Ce(III) 1,1,1,5,5,5-hexafluoro-2,4-pentanedionato diglyme adduct ($Ce(hfa)_3$·diglyme). The X-ray diffraction patterns of all samples grown in the 450−750 °C deposition temperature range point to the formation of ⟨100⟩-oriented CeO_2 films, whereas at higher deposition temperatures (850−1050 °C) all the deposited CeO_2 films show ⟨111⟩ texture. fwhm rocking curves values clearly indicate that the texturing of CeO_2 crystallites is greatly improved upon increasing the deposition temperature in both cases. Typical pole figure patterns demonstrate a cube-on-cube epitaxial growth in the case of ⟨100⟩-oriented CeO_2 films, whereas ⟨111⟩-oriented CeO_2 films show different in-plane alignments of the crystallites. A possible explanation for textural changes is proposed.

Introduction

Major advances have been made in recent years in high-temperature superconductor (HTS) research, resulting in an increasing use of HTS materials in commercial and precommercial power applications[1−3] and electronic devices.[4,5] In particular, HTS films are good candidates for devices adopted in cellular communication areas.[6−9] In this context, rutile (TiO_2) has attracted considerable interest in recent years as a versatile and suitable substrate for fabrication of HTS passive filters. In fact, this substrate possesses a higher dielectric constant with respect to $LaAlO_3$, YSZ, and Al_2O_3 and relatively low loss tangent.[10] The most important point in these applications is the preparation of highly (00*l*)-oriented HTS thin films to achieve superconducting devices with low microwave losses.[11,12]

In the case of HTS applications for electronic and magnetic devices, texturing plays a key role since well-matched and -textured multilayer structures often drive properties and performances as well as increase the device lifetime. Moreover, the growth of epitaxial films currently provides the opportunity to study film and multilayer properties that depend on the orientation of crystalline growth.

Finally, the fabrication of HTS multilayer devices requires lattice-matched, chemically compatible, and thermally stable materials as buffer, dielectric, and/or insulator layers.

Among the numerous oxides often used as buffer layers,[13] epitaxial cerium oxide (CeO_2) thin films are currently of interest for different applications in key areas of thin film technology, ranging from semiconductors[14−16] to superconductors[17,18] and solid oxide fuel cells.[19] In fact, these films are used as protective buffer

* E-mail: lfragala@dipchi.uict.it.
[†] IMM, sezione di Catania, CNR.
[‡] Università di Catania.

(1) Wu, X. D.; Foltyn, S. R.; Arendt, P. N.; Blumenthal, W. R.; Campbell, I. H.; Cotton, J. D.; Coulter, J. Y.; Hults, W. L.; Maley, M. P.; Safar, H. F.; Smith, J. L. *Appl. Phys. Lett.* **1995**, *67*, 2397−2399.
(2) Goyal, A.; Norton, D. P.; Budai, J. D.; Paranthaman, M.; Specht, E. D.; Koreger, D. M.; Christen, D. K.; He, Q.; Saffian, B.; List, F. A.; Lee, D. F.; Martin, P. M.; Klabund, C. E.; Hartfield E.; Sikka, V. K. *Appl. Phys. Lett.* **1996**, *69*, 1795−1797.
(3) Matsumoto, K.; Kim, S. B.; Win, J. G.; Hirabayashi, I.; Watanabe, T.; Unp, N.; Ikeda, M. *IEEE Trans. Appl. Supercond.* **1999**, *9*, 1539−1542.
(4) Terashima, Y.; Yamazaki, M.; Kudo, Y.; Yoshino, H.; Ando, K.; Oshima, S. *Jpn. J. Appl. Phys* **1994**, *33*, L1592−L1594.
(5) Chaloupka, H. J.; Hein, M. A.; Muller, G. *SPIE Proc.* **1994**, *36*, 2156.
(6) Lancaster, M. J. *Passive Microwave Device Applications of High-Temperature Superconductors*; Cambridge University Press: Cambridge, 1997; Chapters 4 and 5.
(7) Hein, M. *High-Temperature-Superconductor Thin Films at Microwave Frequencies*, Springer Tracts in Modern Physics; Springer: Berlin, 1999; Vol. 155, Chapters 3 and 5.
(8) Klaudam, M.; Kasser, T.; Mayer, B.; Neumann, C.; Schnell, F.; Aminov, B.; Baumfalk, A.; Chaloupka, H.; Kolesov, S.; Piel, H.; Klein, N.; Schornstein, S.; Bareiss, M. *IEEE Trans. Microwave Theory Tech.* **2000**, *48*, 1227−1230.
(9) Li, H.; He, Y. S.; He, A. S.; Li, S.; Li, C.; Yon, L.; Liang, J.; Zhu, W.; Zhou, Y.; Hong, J.; Lancaster, M. J. *Supercond. Sci. Technol.* **2002**, *15*, 276−279.
(10) Templeton, A.; Wang, X. R.; Penn, S. J.; Webb, S. J.; Cohen, L. F.; Alford, N. M. *J. Am. Ceram. Soc.* **2000**, *83*, 95−98.
(11) Nerumi, E.; Song, L. W. *Appl. Phys. Lett.* **1991**, *58*, 1202−1204.
(12) Willensen, B. A.; Kilhstrom, K. E.; Dahen, T.; Scalapino, D. J.; Gowe, B.; Bonn, D. A.; Hardy, W. N. *Phys. Rev. B* **1998**, *58*, 6650−6654.
(13) Wordenweber, R. *Supercond. Sci. Technol.* **1999**, *12*, R86−R102.
(14) Cossarutto, L.; Chaoui, N.; Million, E.; Muller, J. F.; Lambert, J.; Alnot, M. *Appl. Surf. Sci.* **1998**, *126*, 352−355.
(15) Jones, J. T.; Bridger, P. M.; Marsh, O. J.; McGill, T. C. *Appl. Phys. Lett.* **1999**, *75*, 1326−1328.
(16) Baue, G.; Song, Y.; Jung, D.; Roh, Y. *Appl. Phys. Lett.* **2000**, *77*, 729−731.

10.1021/cm021348r CCC: $25.00
Published on Web 03/14/2003

layers for HTS growth, owing to the small lattice mismatch with 45° rotated crystallites of HTS films, to similar thermal expansion coefficients,[20] and to their chemical stability.

CeO_2 thin films have been deposited by several techniques including thermal and electron beam evaporation,[21,22] laser ablation,[23] pulsed laser deposition,[24] ion-assisted deposition,[25] and reactive dc magnetron sputtering.[26]

Metal−organic chemical vapor deposition (MOCVD), however, represents a more attractive technique for microelectronic applications since it offers great potentialities for large area growth, good film uniformity, and excellent conformal step coverage at device dimensions less than 2 μm. The majority of MOCVD studies, focused on fabrication of CeO_2 thin films with superior crystalline and morphological quality, have used single-crystal substrates, which show a little lattice mismatch relative to CeO_2 films, such as yttria-stabilized zirconia (YSZ) (5%),[27,28] Al_2O_3 r-plane (5.7% and 12%),[20,29] and Si (0.4%).[30] Generally, for substrates with a reasonable lattice match, operational conditions required for film depositions are relatively substrate-independent. CeO_2 and TiO_2 belong to different space groups. The former has a cubic fluorite-type structure with a lattice parameter $a = 0.5411$ nm, whereas the latter belongs to a tetragonal structure with lattice spacings $a = 0.4593$ nm and $c = 0.2959$ nm. In this case, (001) TiO_2 substrate and (100) CeO_2 thin films are largely mismatched (about 17%).[31] This large difference points to a more critical epitaxial growth than that observed on previously mentioned substrates.

The present study is addressed to find the best deposition conditions for fabrication of high-quality CeO_2 buffer layers on TiO_2. To our knowledge, there have been no previous reports on the growth of CeO_2 on TiO_2 substrates.

CeO_2 thin films have been grown by MOCVD using a volatile metal−organic second-generation precursor, Ce(hfa)$_3$·diglyme [Hhfa = 1,1,1,5,5,5-hexafluoro-2,4-pentanedione, diglyme = $(CH_3O(CH_2CH_2O)_2CH_3)$]. The epitaxy of ⟨100⟩-oriented CeO_2 films has been driven by varying deposition parameters. It has been found that nanocrystalline CeO_2 thin films grow with different crystallographic orientations on rutile substrates upon varying the deposition temperature.

Experimental Section

A horizontal hot-wall MOCVD reactor was used in all experiments. The anhydrous, air, and thermally stable metallorganic source, Ce(hfa)$_3$·diglyme, was prepared as described elsewhere.[32] It was vaporized from the melt at 120 °C. Ar (100 sccm) was used as a carrier gas and 100 sccm water-saturated oxygen flow was fed close to the substrate as the reacting gas. The water bubbler was kept at 25 °C. Fluorine contamination in the films was precluded by adding water vapor into the oxygen stream.[33] Depositions were carried out for 60 min in the reactor chamber maintained at 4 Torr. Deposition temperatures were varied in the 450−1050 °C range. The deposition rate changed from 1.1 μm/h at 450 °C deposition temperature to 0.7 μm/h at 1050 °C. The thicknesses were evaluated by cross-section SEM observations. ⟨001⟩-oriented TiO_2 10 × 10 mm^2 substrates were purchased from Crystal GmbH.

X-ray diffraction measurements (XRD) were recorded on a Bruker-AXS D5005 $\theta-\theta$ X-ray diffractometer, using Cu Kα radiation operating at 40 kV and 30 mA. Rocking curves of the CeO_2 (200) and (111) reflections were measured and used as texturing indicators. A four circle Bruker-AXS D5005 X-ray diffractometer was used to study the CeO_2 films in-plane grain alignment.

Film surface morphologies were examined using a LEO Iridium 1450 scanning electron microscope (SEM). Film atomic composition was determined by wavelength dispersive X-ray analysis (WDX) using an Oxford Instruments WDX-3PC analyzer. The WDX analyses were carried out at 15-kV accelerating voltage, 10-nA current, and 100-s acquisition time. TAP (thallium acid phthalate) and LSM60 (synthetic multilayered structure) crystals were used as an X-ray selector for F and C, respectively.

Results and Discussion

Structural Characterization. Earlier results[32,34] have already shown that the presently adopted Ce(hfa)$_3$·diglyme precursor represents a reliable source for deposition of cerium-containing films due to its low melting point (75 °C), which allows evaporation from the liquid phase. This represents an important issue for MOCVD applications, where liquid source precursors appear the most desirable due to the greater stability of the vapor pressure and to the absence of any effect of crystallite size on the evaporation rate and, hence, on the film growth rate. Even more important, Ce(hfa)$_3$·diglyme adduct produces good quality CeO_2 thin films at a deposition temperature (450 °C) significantly lower than that usually required (>550 °C).[35] This also is an important issue since lower deposition temperatures are highly desirable for multilayer device fabrication.

Initial experiments for growing CeO_2 films over TiO_2 (001) substrates have been attempted at 450 °C. The substrate size is 10 × 10 mm^2 and the films are uniform

(17) Inoue, T.; Yamamoto, Y.; Koyama, S.; Suziki, S.; Ueda, Y. *Appl. Phys. Lett.* **1990**, *56*, 1332−1333.
(18) Tian, Y. J.; Linzen, S.; Schmidl, F.; Matthes, A.; Scheelidewind, H.; Siedel, P. *Thin Solid Films* **1999**, *338*, 224−230.
(19) Inuoe, T.; Setoguchi, T.; Educhi, K.; Arai, H. *Solid State Ion.* **1989**, *35*, 285−291.
(20) Lu, Z.; Hiskes, R.; Di Carolis, S. A.; Nel, A.; Rate, R. K.; Feigelson, R. S. *J. Cryst. Growth* **1995**, *156*, 227−234.
(21) Lee, S.; Oh, D.; Goo, D.; Youm, D. *Thin Solid Films* **1995**, *258*, 299−304.
(22) Inoue, T.; Ohsuna, T. *Appl. Phys. Lett.* **1991**, *59*, 3604−3606.
(23) Yoshimoto, M.; Nagata, H.; Tsukahara, T.; Koinuma, H. *Jpn. J. Appl. Phys.* **1990**, *29*, L1199−L1202.
(24) Nagata, H.; Tsukahara, T.; Gonda, A.; Yoshimoto, M.; Koinuma, H. *Jpn. J. Appl. Phys.* **1991**, *30*, L1136−L1138.
(25) Al-Robaee, M. S.; Naraimha, K.; Mohan, S. *J. Appl. Phys.* **1992**, *71*, 2380−2386.
(26) Granqvist, C. G.; Azens, A.; Hjelm, A.; Kullman, L.; Niklasson, G. A.; Ronnow, D.; Stromme Mattsson, M.; Veszelei, M.; Vaisar, G. *Sol. Energy* **1998**, *63*, 199−216.
(27) Becht, M.; Morishita, T. *J. Alloys Compd.* **1997**, *251*, 310−313.
(28) Belot, J. A.; Wang, A. C.; McNeely, R. J.; Liable-Sanfs, L.; Rheingold, A. L.; Marks, T. J. *Chem. Vap. Dep.* **1999**, *5*, 65−69.
(29) Frohlich, K.; Souc, J.; Machajdik, D.; Jergel, M.; Snauwaert, J.; Hellemans, L. *Chem. Vap. Deposition* **1998**, *6*, 216−220.
(30) Fukuda, H.; Miura, M.; Sakuma, S.; Nomura, S. *Jpn. J. Appl. Phys., Part 1* **1998**, *37*, 4158−4159.
(31) The following notation has been used: [*hkl*] denotes a single direction and ⟨*hkl*⟩ a general set of directions; a plane is labeled as (*hkl*) and a general set of planes as {*hkl*}.
(32) Malandrino, G.; Lo Nigro, R.; Benelli, C.; Castelli, F.; Fragalà, I. L. *Chem. Vap. Deposition* **2000**, *6*, 233−238.
(33) McAleese, J.; Plakatouras, J. C.; Steele, B. C. H. *Thin Solid Films* **1996**, *280*, 152−159.
(34) Lo Nigro, R.; Malandrino, G.; Fragalà, I. L. *Chem. Mater.* **2001**, *13*, 4402−4404.
(35) Wang, A. C.; Belot, J. A.; Marks, T. J.; Markworth, P. R.; Chang, R. P. H.; Chudzik, M. P.; Kannewurf, C. R. *Physica C* **1999**, *320*, 154−160.

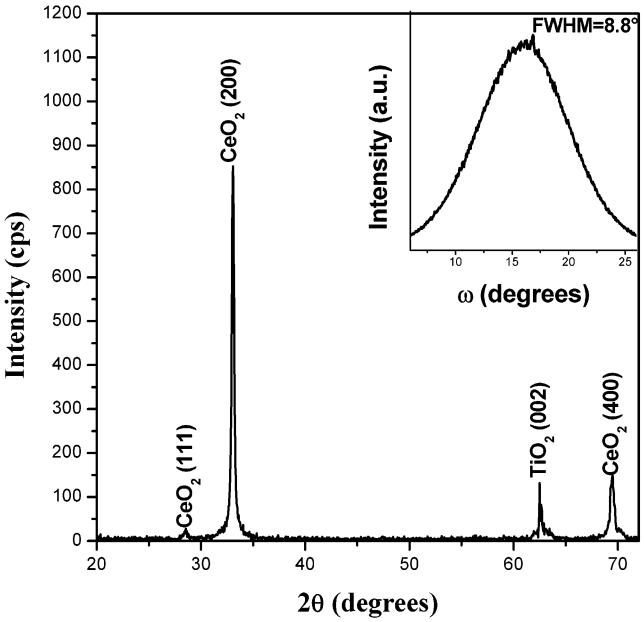

Figure 1. $\theta-2\theta$ XRD scan of a (100) CeO_2 film deposited at 450 °C on TiO_2 (001). The insert shows the rocking curve of the (200) reflection.

all over the surface. The XRD pattern is reported in Figure 1. The presence of peaks at $2\theta = 33.08°$ and 69.4°, related to the (200) and (400) reflections, respectively, indicates that ⟨100⟩-oriented CeO_2 thin films have been obtained on TiO_2 (001) at 450 °C. The rocking curve (see insert in Figure 1) of the (200) CeO_2 reflection has a full-width at half-maximum (fwhm) of about 9°, significantly greater than that found for CeO_2 films deposited on single-crystal substrates at the same deposition temperature.[27,32,35] This effect certainly accompanies the great lattice mismatch with (001) TiO_2 substrates.

To improve epitaxy, several depositions have been attempted in the 450−1050 °C substrate temperature range and the consequent texture evolution has been monitored. In the 450−750 °C temperature range, CeO_2 films are mostly ⟨100⟩ -oriented with an evident gradual change to ⟨111⟩ texturing upon increasing the temperature (Figure 2). In the same range, the fwhm values of the (200) reflection rocking curves (Figure 3) decrease, thus clearly showing that the alignment of CeO_2 films improves significantly. Samples deposited at 750 °C are ⟨100⟩-oriented and show a considerably smaller fwhm value (1.7°). These films contain small quantities of (111)-oriented grains. This represents a recurring problem in the preparation of CeO_2 films by various techniques[36] since the competing growth of ⟨111⟩-oriented domains depends on the deposition temperature. Nevertheless, a small quantity of ⟨111⟩ grains in ⟨100⟩-oriented CeO_2 films is not a critical issue for their use as buffer layers.

Further investigations above 750 °C have shown an intriguing competition between ⟨100⟩ and ⟨111⟩ domains. Films deposited at 850 °C are mostly ⟨111⟩-textured, even though there is evidence of some ⟨100⟩ crystals. The (111) domains become predominant at 1050 °C. Representative $\theta-2\theta$ scans are reported in Figure 2.

(36) Frohlich, K.; Souc, J.; Machajdik, D.; Kobzev, A. P.; Weiss, F.; Senateur, J. P.; Dahmen, K. H. *J. Phys. IV* **1995**, *5*, C5-533−C5-539.

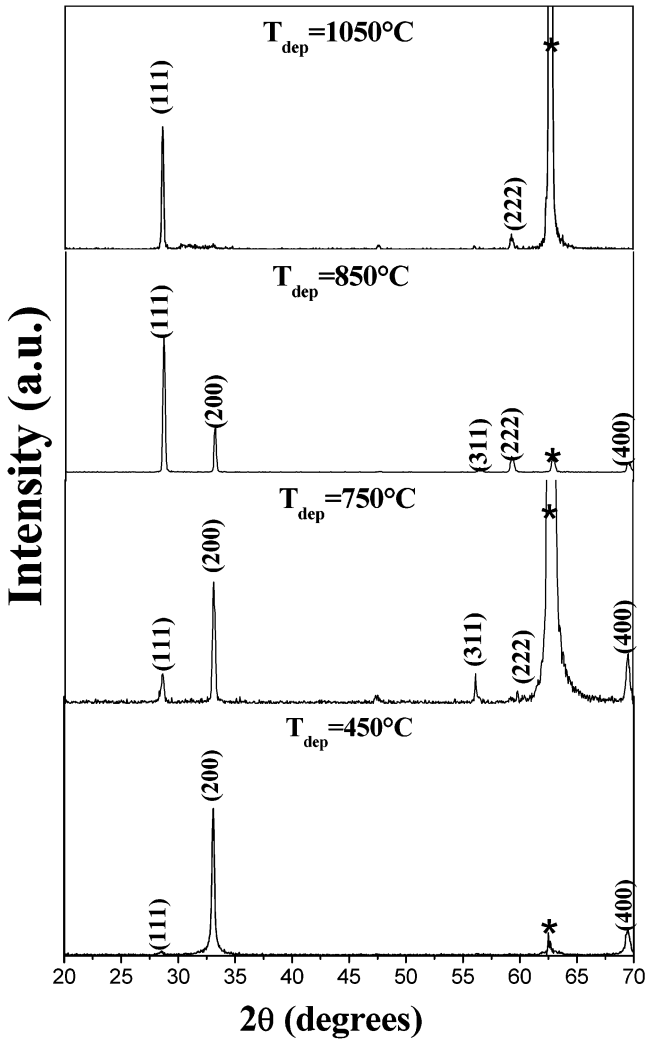

Figure 2. $\theta-2\theta$ XRD patterns of CeO_2 films deposited at various temperatures (450−1050 °C) (* = substrate (002) reflection).

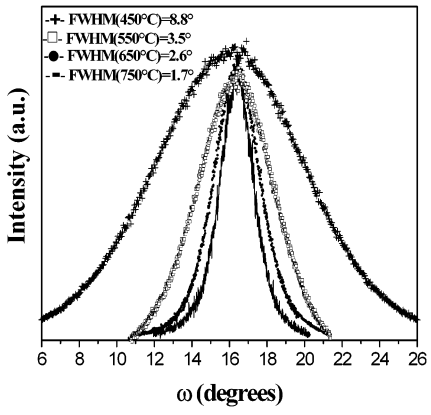

Figure 3. Rocking curves of the (200) reflection of CeO_2 films at various deposition temperatures (450−750 °C).

Rocking curves of the (111) reflection at selected temperatures are shown in Figure 4. There is clear evidence that narrower widths are associated with films deposited at higher temperatures and the smallest fwhm value (0.4°) has been measured at 1050 °C. fwhms measured on both ⟨100⟩ and ⟨111⟩ films generally point to a better texturing in the case of higher deposition temperature. In particular, the ⟨111⟩ CeO_2 films on TiO_2 substrates, prepared at deposition temperature as high

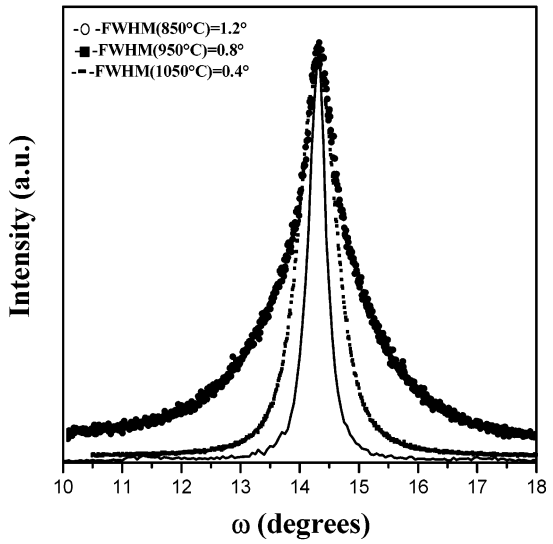

Figure 4. Rocking curves of the (111) reflection of CeO_2 films at various deposition temperatures (850−1050 °C).

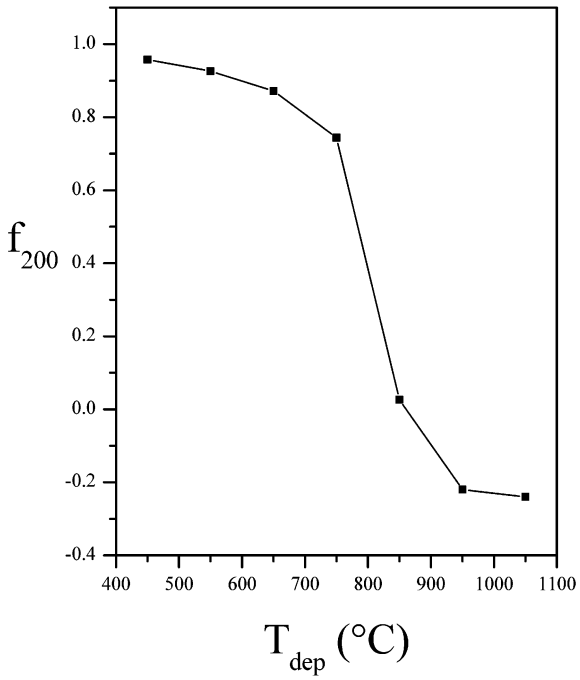

Figure 5. Variation of the degree of (200) preferred orientation (f_{200}) versus deposition temperatures.

as 1050 °C, show an out-of-plane alignment better than ⟨100⟩ CeO_2 films.

The amount of ⟨100⟩ relative to ⟨111⟩ domains can be semiquantitatively evaluated from the plot of the f_{200} parameter (degree of ⟨100⟩ preferred orientation) vs the temperature (Figure 5),

$$f_{200} = (P_{200} - P^0_{200})/(1 - P^0_{200})$$

$$P_{200} = I_{200}/(I_{111} + I_{200})$$

$$P^0_{200} = I^0_{200}/(I^0_{111} + I^0_{200})$$

where I_{hkl} and I^0_{hkl} are the intensities of (hkl) reflections in the present CeO_2 films and in a polycrystalline standard powder sample, respectively. Of course, only the (111) and (200) peaks have been considered since the other peaks have really negligible intensities. Negative values (as in the 900−1050 °C range) of the f_{200} parameter indicate that films are ⟨111⟩ preferentially oriented. At lower deposition temperature (450 °C) CeO_2 films are ⟨100⟩-oriented (i.e., $f_{200} \approx 100\%$). The rocking curve fwhm value points, however, to a poor crystallite alignment. Films deposited at 750 °C are 80% ⟨100⟩-textured with 1.7° fwhm. In the films deposited at 850 °C, the intensity of the (200) reflection is less than 30%, and the grain dispersion is so high that the rocking curve is no more detectable. A further increase of the deposition temperature (950 °C) results in a marked improvement of both ⟨111⟩ texture (95%) and of the out-of-plane crystallite alignment (fwhm = 0.8°). At 1050 °C CeO_2 films are 100% ⟨111⟩-oriented and present the best crystallite alignment (fwhm = 0.4°).

In regard to the film thicknesses, note that the deposition rate decreases on increasing temperature. This is a well-known issue since precursor depletion occurs at higher temperature due to its decomposition on the reactor walls. Nevertheless, there is no doubt that different growth rates might also depend on the different orientations.

In-Plane Texture Analysis. In this context, it becomes of interest to understand the epitaxy of CeO_2 films and, in particular, whether the heterostructure CeO_2/TiO_2 is in-plane-oriented. The pole figures, plotted in the 0°(center) < ψ < 90° (rim) range of the distance of the pole angle, are reported in parts a and b of Figure 6. Figure 6a shows the pattern of ⟨100⟩ CeO_2 thin films deposited at 750 °C. The 2θ angle has been fixed at 28.54° (corresponding to CeO_2 (111) reflection) to record the pole figure. Four diffraction peaks, 90° spaced in φ, have been observed at $\psi = 54.5°$ with a 4-fold symmetry, showing, as expected for a cubic structure, that the CeO_2 {111} planes are 54.75° tilted with respect to the CeO_2 {100} planes, which lie parallel to the substrate surface. The four peaks, 90° spaced, clearly point to a good in-plane orientation. The central peak corresponds to the ⟨111⟩-oriented grains as observed in the X-ray pattern (Figure 2).

The epitaxial relationship between the ⟨111⟩-oriented CeO_2 films and ⟨001⟩ TiO_2 substrate has been studied as well. In the case of ⟨111⟩-oriented CeO_2 thin films, deposited at 1050 °C, the related pole figure has been recorded using a 2θ angle of 33.08°, corresponding to the (200) reflection. Twelve equally spaced (every 30°) peaks at $\psi = 54.6°$ and one peak at $\psi = 0°$ have been observed, instead of the three peaks expected for the ⟨100⟩ directions. This indicates that the ⟨111⟩ CeO_2 films consist of, at least, two sets (vide infra) of crystallites, each rotated by 90° in the substrate plane. In addition, crystallites are probably twinned about the [111] direction, as expected for a face-centered cubic crystal.[37] On the basis of the cubic symmetry of this lattice, crystal growth could even involve four sets of twinned crystallites with the consequence that, for more than two crystallite in-plane orientations, various X-ray reflections could coincide. An obvious consequence, therefore, is that the exact number of distinct crystallite orientations cannot be determined. In Figure 7 a schematic

(37) Kelly, A.; Groves, G. W. *Crystallography and Crystal Defects*; Addison−Wesley: Reading, MA, 1970.

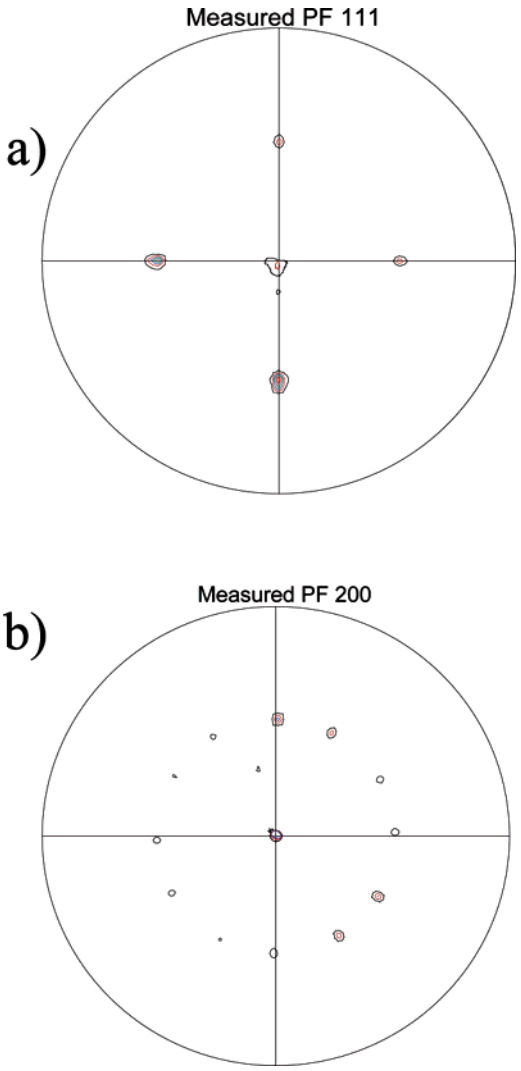

Figure 6. Pole figures of (a) ⟨100⟩-oriented CeO_2 films deposited at 750 °C, using the (111) reflection as the pole; (b) ⟨111⟩-oriented CeO_2 films deposited at 1050 °C, using the (200) reflection as the pole.

representation of the CeO_2 (111) and TiO_2 (001) planes is reported. If we consider the CeO_2 [−110] direction, which lies in the (111) plane, two epitaxial in-plane variants are possible. One alignment arises when the CeO_2 [−110] direction is parallel to the TiO_2 [010] (Figure 7a) and the second derives by a 90° CeO_2 cell rotation around the [111], with a consequent alignment of the CeO_2 [−110] with the TiO_2 [100] (Figure 7b).

Identical behavior has already been reported for other heteroepitaxial pairs, such as (111) $BaTiO_3$ || (001)YSZ[38] or (111) $LaAlO_3$ || (001) YSZ.[39]

Additional information about the in-plane relationship of CeO_2 films relative to the underlying TiO_2 substrate can be obtained from Φ-scans of the CeO_2/TiO_2 film/substrate system (Figure 8). Φ-scans of ⟨100⟩-oriented CeO_2 film on a (001)TiO_2 substrate have been recorded using as poles the CeO_2 (111) reflection ($2\theta = 28.54°$) and the TiO_2 (111) reflection ($2\theta = 41.22°$) at ψ tilt angles of 54.75° and 42.24°, respectively. The two

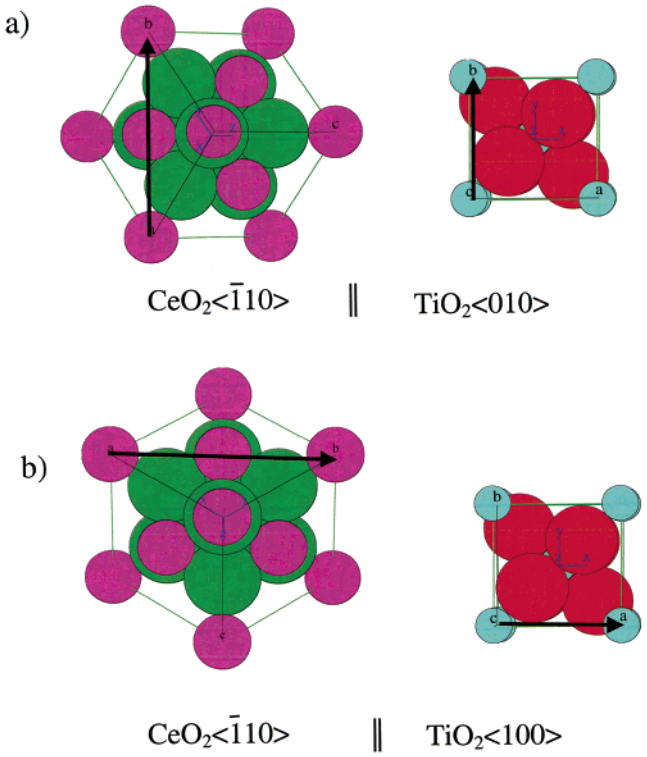

Figure 7. Model of cell lattice matching for a (111) CeO_2 film and (001) TiO_2 substrate planes. Epitaxial relations are as follows: CeO_2 (111) || TiO_2 (001), CeO_2 ⟨−110⟩ || TiO_2 ⟨100⟩; CeO_2 (111) || TiO_2 (001), CeO_2 ⟨−110⟩ || TiO_2 ⟨010⟩.

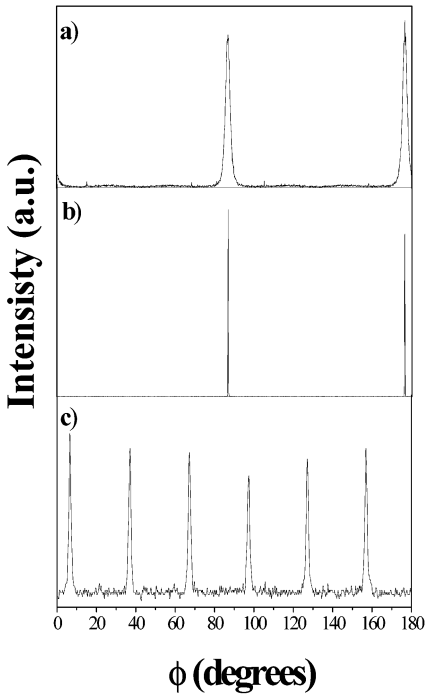

Figure 8. Φ-scans using the (111) or (200) CeO_2 reflection as the pole for cerium dioxide films and the (111) TiO_2 reflection for a rutile substrate: (a) ⟨100⟩-oriented CeO_2 films; (b) ⟨001⟩ TiO_2 substrate; (c) ⟨111⟩-oriented CeO_2 films.

peaks from the CeO_2 {111} planes are coincident with the {111} TiO_2 Φ positions. This clearly demonstrates that the CeO_2 unit cell is not rotated in the plane with respect to the TiO_2 substrate; thus, the [100] and [010] axis directions are aligned for the film and the substrate (i.e., CeO_2 ⟨100⟩ || TiO_2 ⟨100⟩).

(38) Gorbenko, O.; Graboy, I. E.; Novozhilou, M. A.; Kaul, A. R.; Wahl, G.; Svetchnikov V. L. *J. Phys. IV* **2001**, Pr3/247−Pr3/254.
(39) Molodyk, A. A.; Korsakov, I. E.; Novojilov, M. A.; Graboy, I. E.; Andrey, R. K. *Chem. Vap. Deposition* **2000**, *6*, 133−138.

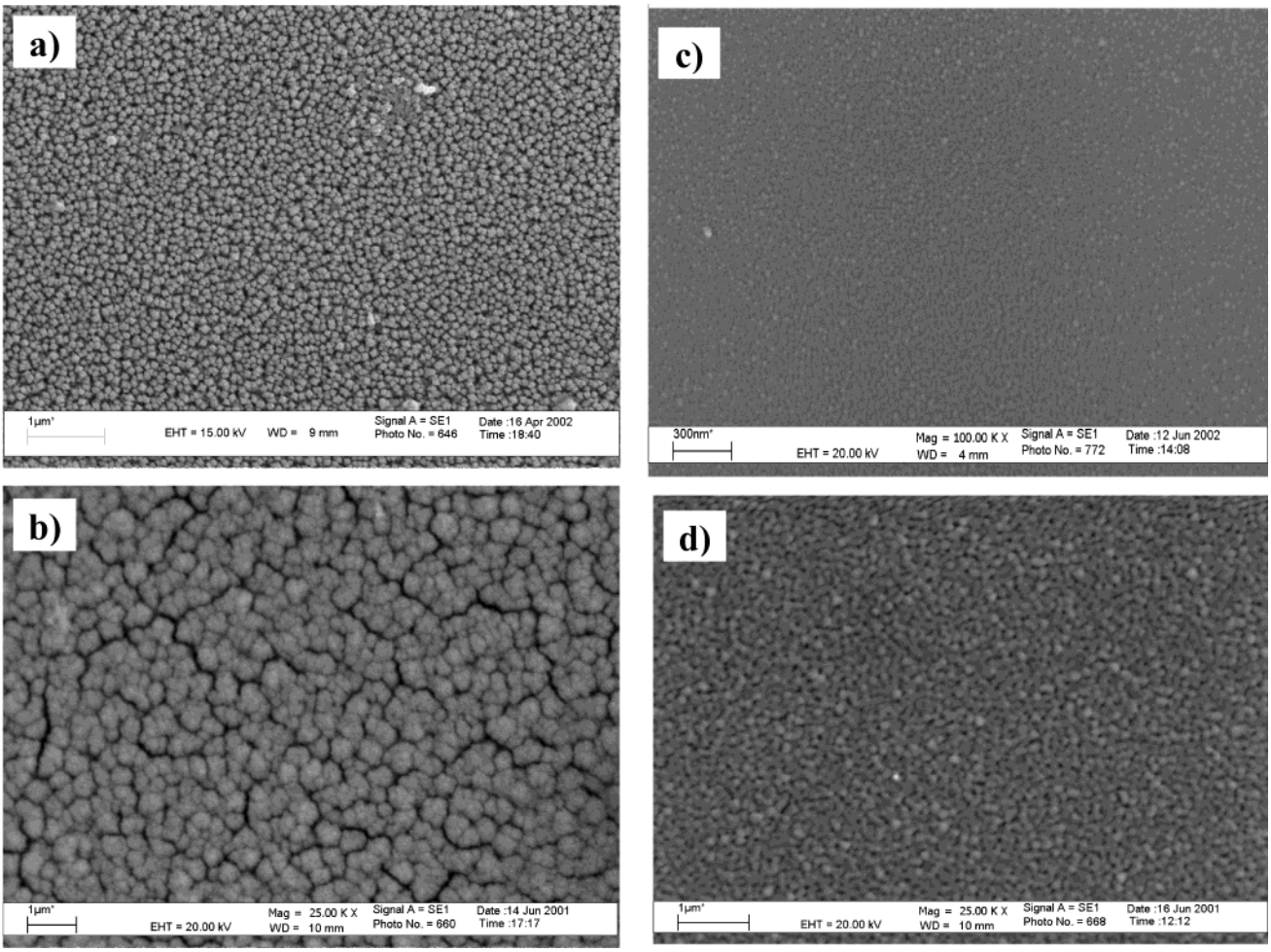

Figure 9. SEM images of surface morphologies of ⟨100⟩ CeO_2 epitaxial films deposited at (a) 450 °C, (b) 750 °C, (c) 750 °C and slowly cooled, and of ⟨111⟩ CeO_2 epitaxial films deposited at 1050 °C (d).

Similarly, the Φ-scan of the CeO_2 (200) peak in a pure ⟨111⟩ film is displayed in Figure 8c. Of course, instead of the three peaks expected for the (200) reflection at $\psi = 54.75°$, 12 equally spaced (30°) peaks are again present.

The in-plane mosaic spread of both ⟨100⟩ and ⟨111⟩ orientations of CeO_2 films has been estimated from fwhm values of the Φ scan peaks. Differences in the angular spreading are evident for the ⟨111⟩ and ⟨100⟩ textures. In the former case, the Φ scan fwhms are quite small (∼1.17°) and, in any case, slightly higher than the mosaicity of the films measured by the rocking curves. Broader distributions (close to 2°) were measured for the ⟨100⟩ texturing. The broadening of ΔΦ observed in ⟨100⟩-oriented films, larger than that in ⟨111⟩, can be due to the elastic strain caused by the lattice mismatch. Note, however, that the epitaxial quality of present (100) CeO_2 films is comparable to that previously observed for CeO_2 films deposited by MOCVD on single-crystal substrates[40] having a lattice mismatch greater than 5%.

The cube-on-cube epitaxial growth of the ⟨100⟩ CeO_2 films on TiO_2 occurs despite the large mismatch. Such a difference certainly causes a sizable distortion of the CeO_2 cell for lattice matching epitaxy. In particular, the ⟨100⟩-oriented films, whose [001] and [010] directions lie in-plane, have single-unit cell lattice mismatch of 17%. This mismatch, however, can be greatly reduced by matching five unit cells of CeO_2 to six unit cells of TiO_2. In this case the mismatch is 1.8%. Although this model implies a large number of Ce atoms are not coincident with the substrate sites, the small distortion allows this domain epitaxy.

For ⟨111⟩-oriented growth, the in-plane lattice directions are [−110] and [11−2]. For the [−110] direction, simple unit cell matching results in a strain of 50%, which can be reduced to 1.9% by matching one unit cell of CeO_2 to two unit cells of TiO_2. For the [11−2] direction, a 1:1 lattice ratio results in a mismatch of 17%. However, by matching six unit cells of TiO_2 to five of CeO_2 along this direction, the mismatch is only 1.8%.

Simple lattice mismatch considerations could suggest that the ⟨111⟩ orientation should be preferred to the ⟨100⟩, due to the slightly smaller lattice mismatch with the substrate and to the lower surface energy for a face-centered cubic (fcc) structure.[41] The reason for the occurrence of both ⟨100⟩ and ⟨111⟩ orientations of CeO_2 films is not fully understood. Nevertheless, a suitable rationale can be found in analogy to the case of CeO_2 films grown on random substrates, such as Hastelloy

(40) Inagaki, T.; Yoshimura, Y.; Kanda, Y.; Matsumoto, Y.; Minami, K. *Nucl. Instrum. Methods A* **2000**, *443*, 126−135.

(41) Schowalter, L. J.; Fathauer, R. W.; Goehner, R. P.; Turner, L. G.; De Blois, R. W.; Hashimoto, S.; Peng, J. L.; Giboon, W. M.; Krusius, J. P. *J. Appl. Phys.* **1985**, *58*, 302−306.

C276 and polycrystalline YSZ.[34] In those cases, ⟨100⟩-oriented CeO_2 films were grown in a homologous temperature ($T_h = T_{dep}/T_{melting}$) range[42] in which the fiber texture can be rationalized by a model for texture development based on a subtle balance between differences of surface energies and elastic energies of differently oriented grains.[43] For example, for a fcc film, the ⟨111⟩ orientation is favored by surface energy, even though in the mentioned deposition temperature range some modifications to the ⟨100⟩ texturing can be induced by the different elastic energy stored in grains with different orientations. At higher deposition temperatures, when crystallites are formed under higher surface mobilities, it is reasonable to assume that lattice match could play a more important role in determining the preferential orientation.

Note, however, that the reason for the occurrence of both ⟨100⟩ and ⟨111⟩ orientations cannot be fully rationalized, and in addition, there are no other results to be compared with present data since to our knowledge CeO_2 films have never been grown on TiO_2.

Morphological Characterization. The film surface has been investigated by scanning electron microscopy (SEM). The CeO_2 films exhibit a surface structure consisting of grains with different shapes and size depending on both deposition temperatures and different structural orientations. Two grain types can be distinguished: (i) nanostructured grains with rounded shape and (ii) pyramidal caps with a more random shape.

The SEM image of a ⟨100⟩-oriented CeO_2 film, deposited at 450 °C, is shown in Figure 9a. The morphology consists of well-connected pyramidal-shaped grains with a diameter of 100 nm. These regularly shaped grains grow oriented in the [100] direction and they are capped by pyramids, the four triangular faces being {111} planes. There is some evidence of the same morphology from previous studies on the growth of ⟨100⟩-oriented CeO_2 film on a random Hastelloy C276 substrate.[34]

The SEM image of ⟨100⟩-oriented CeO_2 film deposited at 750 °C shows a cracked surface (Figure 9b). Crack formation may be associated with stress in the CeO_2 layers. This is possibly due to the lattice mismatch between CeO_2 films and TiO_2 substrates and/or to different thermal expansion coefficients. On the other hand, this problem has been overcome by a slow cooling (3 °C/min) of CeO_2 films under vacuum. The surface morphology of a slowly cooled sample is shown in Figure 9c. The nanostructured surface consists of few tens of nanometer wide grains, forming a smooth and homogeneous surface suitable for the growth of superconducting thin films.

In Figure 9d is reported the SEM image of a ⟨111⟩-oriented film deposited at 1050 °C. The sample presents a different morphology which consists of a fine-grained structure and rounded grains having diameters of about 100 nm. The grains form a regularly and tightly packed array, indicating a good in-plane and out-of-plane alignment.

Finally, it is likely that there is no influence of the film thickness, since it varies only from 0.7 to 1.1 μm, on the surface morphology.

The chemical purity of the samples has been determined by wavelength-dispersive X-ray (WDX) analyses. All the experiments on present films indicate negligible C (0.2%) and F (0.1%) contamination. The WDX detection limits are about 200 and 400 ppm, respectively, under the conditions reported in the Experimental Section.

Conclusions

In the present study we report results of cerium dioxide epitaxial deposition on rutile as a potential buffer layer for superconducting films growth. The significant lattice mismatch (about 17%) between a ⟨100⟩-oriented CeO_2 film and TiO_2 (001) substrate points to a critical epitaxial growth. Present data, however, show that epitaxial ⟨100⟩ CeO_2 films can be grown on (001)-oriented TiO_2 substrates by the MOCVD technique.

It has been found that texturing and epitaxy of CeO_2 films is very sensitive to the deposition temperature. The epitaxial growth of ⟨100⟩-oriented CeO_2 films has been tailored by varying deposition parameters and monitored by a complete structural characterization. $\theta-2\theta$ scans and X-ray pole figures show that ⟨100⟩ CeO_2 films with good crystallinity can be epitaxially deposited on (001) TiO_2 substrates in the 450−750 °C temperature range.

Detailed information has been obtained from the related rocking curves whose fwhms indicate that higher temperature values improve the out-of-plane alignment. The ⟨100⟩-oriented CeO_2 films grow cube-on-cube on the TiO_2 substrate, that is, CeO_2 ⟨100⟩ || TiO_2 ⟨100⟩.

Moreover, CeO_2 films, grown at deposition temperatures higher than 750 °C, show a ⟨111⟩ orientation. Pole figures of the (200) reflection for ⟨111⟩ CeO_2 films show 12 maxima, indicating the presence of at least two in-plane variants.

The evolution of fiber texture, upon varying the growth conditions, has been interpreted in terms of surface mobility and lattice matching.

Acknowledgment. The authors thank the Consiglio Nazionale delle Ricerche (CNR) and the MIUR under Progetto Cluster 14 P.E.2. for financial support.

CM021348R

(42) Machlin, E. S. *Materials Science in Microelectronics*; Gyro: New York, 1995.

(43) Bunshah, R. F.; Blocher, J. M., Jr.; Mattox, D. M. *Deposition Technologies for Films and Coating*; Noesy Publication: Park Ridge, NY, 1982.